Journal of Neuropathology and Experimental Neurology
Vol. 60, No. 8
August, 2001
pp. 753–758

Plaque-Induced Abnormalities in Neurite Geometry in Transgenic Models of Alzheimer Disease: Implications for Neural System Disruption

RICKY LE, BA, LUIS CRUZ, PHD, BRIGITA URBANC, PHD, ROGER B. KNOWLES, PHD, KAREN HSIAO-ASHE, MD, PHD, KAREN DUFF, PHD, MICHAEL C. IRIZARRY, MD, H. EUGENE STANLEY, PHD, AND BRADLEY T. HYMAN, MD, PHD

Abstract. Neurites that pass through amyloid-ß deposits in Alzheimer disease (AD) undergo 3 changes: they develop phosphorylated tau immunoreactivity; the density of SMI-32-positive dendrites diminishes; and they also develop a marked alteration in their geometric features, changing from being nearly straight to being quite curvy. The extent to which the latter 2 phenomena are related to phosphorylated tau is unknown. We have now examined whether amyloid-ß deposits in APP695Sw transgenic mice, which have only rare phosphorylated tau containing neurites, develop these changes. We found that dendritic density is diminished within the boundaries of amyloid-ß plaques, with the greatest loss (about 80%, $p < 0.001$) within the boundaries of thioflavine S cores. Remaining dendrites within plaques develop substantial morphological alterations quantitatively similar to those seen in AD. A statistically significant but smaller degree of change in geometry was seen in the immediate vicinity around plaques, suggesting a propagation of cytoskeletal disruption from the center of the plaque outward. We examined the possible physiological consequences of this change in dendritic geometry using a standard cable-theory model. We found a predicted delay of several milliseconds in about one quarter of the dendrites passing through a thioflavine S plaque. These results are consistent with previous observations in AD, and suggest that thioflavine S-positive amyloid-ß deposits have a marked effect on dendritic microarchitecture in the cortex, even in the relative absence of phosphorylated tau alterations.

Key Words: Alzheimer disease; Modeling; Neural networks; Senile plaque; Transgenic.

INTRODUCTION

Amyloid-ß deposits occupy as much as 10% of the surface area of the cortex in an average Alzheimer disease (AD) brain (1). Although there is a consensus that this deposition is at the heart of the disease process, the mechanism whereby amyloid deposition impacts brain function remains uncertain. We have recently demonstrated that amyloid-ß deposits in brains of AD patients cause a diminution in the density of dendrites within their microenvironment, and that remaining dendrites that course through amyloid deposits have an increased likelihood of containing phosphophorylated tau (2). More recently, we employed new quantitative measures of dendritic morphology to determine that remaining phosphophorylated tau-negative neurites that pass through plaques frequently show substantial change in their morphology (an increase in end-to-end distance ratios and curvilinear geometry) (3). Together these results suggest that at least one of the mechanisms by which amyloid deposition alters neuronal function is by local disruption of the neuropil.

One limitation of these studies is that in AD, extensive neuronal loss, neurofibrillary tangles, and extensive neuropil threads could each contribute to dendritic alterations, and the exact role of amyloid-ß deposits is therefore difficult to ascertain with certainty. Here we use 2 mouse models of amyloid-ß deposition—Tg2576 (APPSw) (4) and APPSwX M146L PS1 (PSAPP) (5)—to test the hypothesis that amyloid-ß deposits directly alter dendrites in the neuropil. Neither model displays global neuronal loss or more than rare phosphorylated tau-positive neurites (6, 7). In both models, we demonstrate that thioflavine S-positive plaques (to a greater extent than thioflavine S-negative amyloid-ß deposits) are associated with a local decrease in the density of dendrites, and that there is a marked alteration of the geometry of dendrites that pass through or near thioflavine S plaques. The degree of alterations in measures of dendrite geometry is related to a dendrite's spatial relationship to a plaque. Dendrites that are within the boundaries of a thioflavine S stained deposit are most affected. Importantly, dendrites in the immediate vicinity of thioflavine S plaques are also altered, suggesting that the change in dendritic morphology propagates beyond the borders of the amyloid-ß deposit. Taken together, these results argue that amyloid-ß deposits, and especially thioflavine S amyloid-ß deposits, are sufficient to cause major alterations in the dendritic microarchitecture independent of phosphorylated tau and neuronal disruption seen in AD.

MATERIALS AND METHODS

Transgenic Mice

Hemizygous transgenic mice expressing mutant human APPSw (4) and hemizygous mice expressing a mutant human

From the Department of Neurology (RL, MCI, BTH), Massachusetts General Hospital, Charlestown, Massachusetts; Center for Polymer Studies and Department of Physics (LC, BU, HES), Boston University, Boston, Massachusetts; Department of Biology (RBK), Drew University, Madison, New Jersey; Department of Neurology (KH-A), University of Minnesota, Minneapolis, Minnesota; Dementia Research (KD), Nathan Kline Institute, Orangeburg, New York.

Correspondence to: Bradley T. Hyman, MD, PhD, Alzheimer Disease Research Laboratories, 149 13th Street, Room 6405, Charlestown, MA 02219.

Supported by NIH AG08487 and AG 15453, and a grant from the Adler Foundation (to B.U.).

PS-1 M146 (5) were crossed to generate offspring with 4 genotypes: nontransgenic (non-tg); PS-1; APPSw; and PSAPP. These mice were studied at 12 months of age.

Mice were killed under ether anesthesia and the brains fixed in 4% paraformaldehyde. Forty-μm-thick coronal sections were obtained on a freezing sledge microtome and subsequently stored in 15% glycerol at −20° until used.

Immunohistochemistry

Free-floating sections were permeablized with 0.5% triton X100 in 0.05 molar Tris buffered saline, blocked in 3% nonfat dry milk in Tris buffered saline pH 7.4, and sequentially labeled with primary antibodies against amyloid-ß (R1282, Dr. Dennis Selkoe, Brigham and Women's Hospital, Boston, MA) and SMI32 (1:1,000, Sternberger Monoclonals, Baltimore, MD). Cy3 and Cy5 conjugated secondary antibodies (Jackson Immunoresearch, West Grove, PA) were used. Some sections were counterstained with 0.1% thioflavine S.

Confocal Microscopy

Confocal images were obtained on a laser-scanning confocal microscope (MRC1024, Bio-Rad, Hercules, CA) utilizing a krypton-argon laser with excitation wavelengths of 488 nm, 568 nm, and 647 nm. Images were obtained from frontal cortex (S1BF and S1TR) dorsal to the anterior portion of hippocampal field CA1. Three-dimensional reconstruction of images was taken from 7 sequential Z series, each 0.2-μm thick (100× 1.4 NA oil immersion objective). The three-dimensional image was then projected for analysis as described in our study of AD (3).

Characterization of Morphological Characteristics of Dendrites

Dendritic geometry was characterized by marking the dendrites, and recording their location with regard to the presence of β-amyloid immunostaining or thioflavine S staining. The mean curvature and end-to-end length measures were obtained as previously described using a custom-designed software program (see http://polymer.bu.edu/~ccruz/AD/dendrite-curvature/curv_index.htm/). A running window technique was used to correct for different dendritic lengths. Each dendrite was examined as a set of n-segments, each of which was approximated as a straight line.

Neuronal Network Simulations

We used the Genesis (8) computer model to determine whether an increase in the length of dendrite would affect spike timing from a synaptic input. For these computations we used R_m= 100 Kohmcm^2, R_a = 300 Kohmcm, and C_m = 1 μF/cm^2 (R_a, axial resistance; R_m, membrane resistance; C_m, membrane capacitance). These parameters were chosen to match our previous studies of Alzheimer plaques (3).

Statistical Analysis

Comparisons were by *t*-test (for SMI-32 ratios) or by ANOVA with Kruskal Wallis post-hoc test.

RESULTS

Triple Label Fluorescent Confocal Microscopy

Four groups of animals were studied at 12 months of age: nontransgenic littermate control animals; animals singly transgenic for mutant presenilin-1 (M146L); animals singly transgenic for APPSw; and animals doubly transgenic with both the mutant presenilin and mutant APP genes (PSAPP). The APPSw developed amyloid deposits and thioflavine S-positive amyloid deposits by 12 months of age throughout multiple cortical regions. As previously reported, the PSAPP mice develop enhanced levels of amyloid-ß deposition, the formation of thioflavine S-positive plaques, but only very rare AT-8 phosphorylated tau immunopositive neurites and no neurofibrillary tangles.

Forty-μm-thick frozen sections were immunostained for SMI-32, a nonphosphorylated neurofilament antibody that recognizes the soma and dendritic harborizations of large projection neurons (Sternberger Monoclonals), and R-1282, a polyclonal antibody against amyloid-ß. Some sections were also counterstained with thioflavine S to visualize dense core amyloid deposits (Fig. 1). Neurofilament-positive dendrites were observed to pass through plaques although qualitatively the density of SMI-32-positive dendrites in a plaque appeared to be less than the density of these dendrites in this neuropil. To assess this quantitatively, we compared the percent area covered by SMI-32-positive dendrites in a plaque to the percent area covered by SMI-32-positive processes in the surrounding field. When we looked at all amyloid-ß deposits, we found that there was a diminution of SMI-32 density within the amyloid-ß on the order of 20%–40% (Table 1) that reached statistical significance only in the APPSw mice. However, the subset of amyloid-ß plaques that are thioflavine S-positive had a much more striking alteration: approximately 80% diminution in SMI-32 immunoreactivity within the boundaries of thioflavine S deposits ($p < 0.001$, both APPSw and PSAPP mice).

Amyloid-β Deposits Disrupt Dendritic Geometry

In addition to an absolute loss of SMI-32-positive dendrites, the dendrites that crossed the plaques appeared to be abnormal. We applied the same quantitative morphologic measures we had earlier used for measuring dendritic abnormalities in plaques in AD brain to the current analyses (3). The 2 quantitative methods measure the amount of curvature, a variable that ranges from zero (absolutely straight) to infinity (i.e. 1/radius of an infinitely small circle), and relative length (R_0), which is the ratio of the end-to-end distance of a neurite, compared to its actual curvilinear length. R_0 ranges from zero for a maximally prolonged traverse to 1.0 if the length traversed by the dendrite is the same length as the end-to-end distance.

We next examined the curvature and relative length parameters for dendrites within Aß deposits, within the immediate periphery of amyloid-ß deposits (within 15-μm radial distance from the surface of a plaque), and in the neuropil farther away from an amyloid-ß deposit.

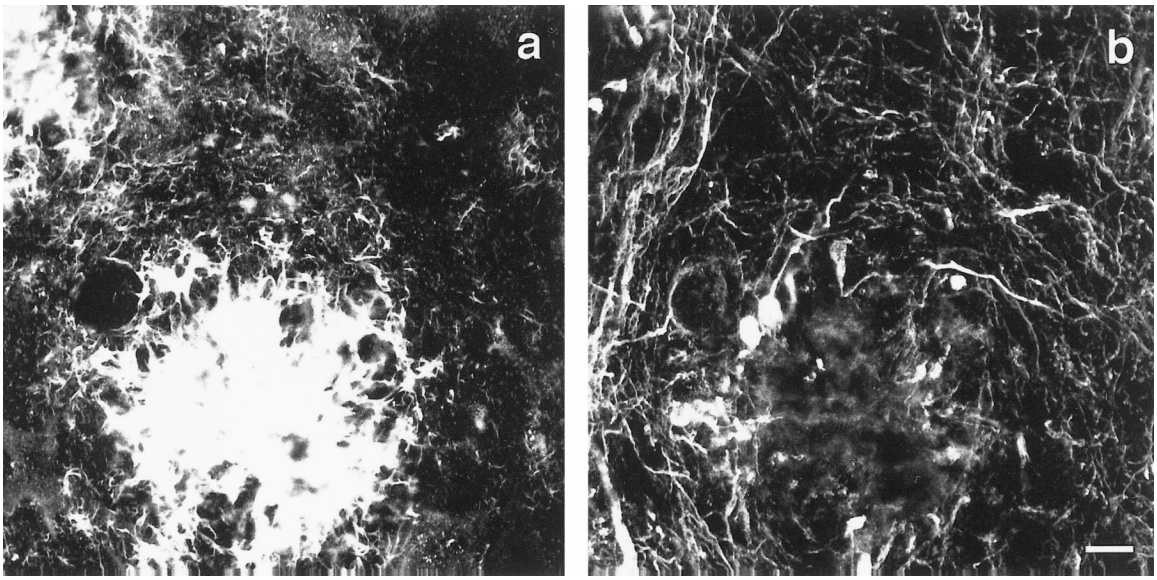

Fig. 1. Confocal photomicrograph of a senile plaque in a PSAPP mouse cortex, immunostained with anti-amyloid-ß (a) or SMI-32 for nonphosphorylated neurofilaments (b). Scale bar = 10 μm.

TABLE 1
SMI-32 Immunoreactivity within Amyloid-β Deposits

Aβ immunoreactive deposits	% of Control	Thioflavine S positive
APP	63 ± 30*	21 ± 10**
PSAPP	81 ± 50	21 ± 10**

Mean ± SD
*$p < 0.05$.
**$p < 0.001$.

Twenty to 25 plaques were identified on confocal micrographs from triple labeled sections either by R1282 immunoreactivity (all Aβ deposits) or by thioflavine S staining from each of four 12-month-old APP or PSAPP cases. An area of approximately equal size, located more than 50 μm away from any amyloid-β channel containing SMI-32 immunoreactivity was also identified and optical density measured. The ratio of SMI-32 pixel density within the boundaries of the plaque to the area outside of the plaque was calculated for each plaque.

Similar studies were performed for thioflavine S-positive plaques. In nontransgenic animals and singly transgenic PS-1 animals, dendrites are quite straight, with curvature close to 0.1 μm^{-1} and R_0 above 0.95. However, in APPSw and PSAPPSw animals, marked changes in dendrite morphology were observed. There was a progressive change in the curvature and R_0 values, with the most severe changes occurring within the boundaries of the thioflavine S-positive plaques, (Tables 2, 3). More subtle (but statistically significant) alterations also occurred in the immediate vicinity of plaques, suggesting a propagation of the cytoskeletal disruption beyond the region occupied by the thioflavine S or amyloid-ß deposit.

Examination of Tables 2 and 3 suggests that the thioflavine S subpopulation of plaques is associated with the most severe changes. It should be noted that the PSAPP mice show essentially the same type and degree of changes as the APPSw mice, except that there are a greater number of thioflavine S-positive plaques in the PSAPP mice. These data are consistent with the idea that the most severe disruption is within the thioflavine S-positive region, a less severe disruption occurs in amyloid-ß deposits that are not thioflavine S-positive, and a modest but still detectable disruption in dendritic architecture occurs in the neuropil immediately surrounding plaques.

Modeling Functional Effects of Neurite Alterations Suggests Potential Disruption of Spike Timing Properties Due To Thioflavine S Plaques

We next examined the possible physiological consequences of the altered dendritic geometry. Using the standard cable-theory model provided by the GENESIS computer model and simulations based on the data of Yuste and Tank (9), we examined whether the change in neurite length would affect spike timing. Neurites that are ''curvy'' (i.e. have a small R_0) traverse a longer path to travel the same linear distance as an unaffected, straight neurite. In the GENESIS model, increased length results in a prolongation of spike timing. As one example of how the changes we observe in neurite architecture would be reflected in this model, we calculated the percent of neurites in each anatomical compartment that are more than 2 standard deviations away from the mean of a normal neurite ($R_0 < 0.82$). In this example, we calculate that neurites that are longer than the average by more than 2 standard deviations have a prolongation of spike timing by 30%. As expected, only about 3% of normal neurites (neurites not associated with plaques) fall in this category, but 27% of dendrites within thioflavine S-positive

TABLE 2
Changes in Dendritic Curvature near Plaques

	Location	Amyloid-β immunoreactive	Curvature (μm^{-1})	Thioflavine S positive
Nontransgenic	—		0.09 ± 0.07 (669)[1]	
PS1	—		0.10 ± 0.07 (725)	
APPSw	in	0.21 ± 0.12 (345)*		0.32 ± 0.15 (36)*+
	peri	0.18 ± 0.11 (521)*		0.21 ± 0.12 (157)*
	out	0.16 ± 0.09 (586)*		0.16 ± 0.08 (154)*
PSAPP	in	0.16 ± 0.11 (518)*		0.31 ± 0.18 (139)*+
	peri	0.14 ± 0.10 (696)*		0.19 ± 0.11 (469)*+
	out	0.13 ± 0.10 (497)*		0.16 ± 0.09 (293)*

[1] mean ± SD (n). *p < 0.001 compared to nontransgenic. +p < 0.001 compared to amyloid-β immunoreactive plaques. Locations: in = within plaque; peri = adjacent to plaque; out = remote from plaque.

TABLE 3
Changes in Dendritic End-to-End Distance Near Plaques

	Location	Amyloid-β immunoreactive	R_0	Thioflavine S positive
Nontransgenic	—		0.96 ± 0.07 (669)[1]	
PS1	—		0.96 ± 0.07 (725)	
APPSw	in	0.92 ± 0.10 (345)*		0.85 ± 0.15 (36)*+
	peri	0.94 ± 0.07 (521)		0.92 ± 0.10 (157)*
	out	0.95 ± 0.07 (586)		0.96 ± 0.04 (154)
PSAPP	in	0.95 ± 0.08 (518)		0.88 ± 0.11 (137)*+
	peri	0.96 ± 0.07 (696)		0.93 ± 0.07 (469)*
	out	0.96 ± 0.06 (497)		0.95 ± 0.05 (293)

[1] mean ± SD (n). *p < 0.001 compared to nontransgenic. +p < 0.001 compared to amyloid-β immunoreactive. Locations: in = within plaque; peri = adjacent to plaque; out = remote from plaque.

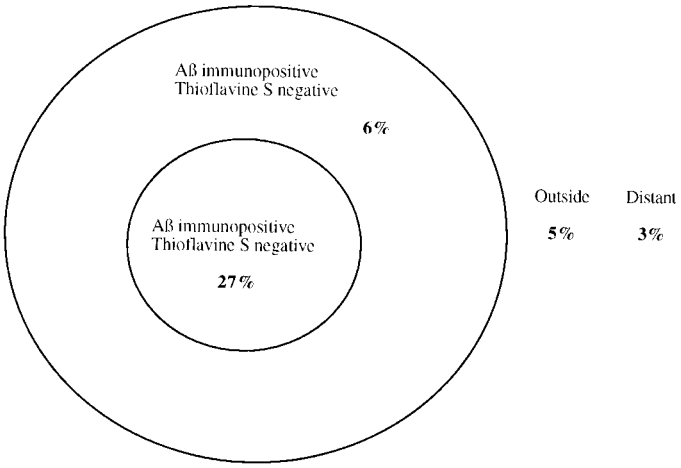

Fig. 2. Schematic diagram illustrating the percent of neurites with a measured $R_0 < 0.82$ (i.e. more than 2 standard deviations from the mean of normal neurites) in each anatomical compartment. See text for details.

regions of plaques are abnormal to at least this degree (Fig. 2). Surprisingly, subtle changes in R_0 also are evident in the region immediately surrounding the thioflavine S core, including neurites within the amyloid-ß-immunoreactive, thioflavine S-negative ''rim'' of plaques, and in the area immediately surrounding plaques (6% and 5%, respectively).

DISCUSSION

Our previous studies of AD cortex led us to the conclusion that neuritic plaques cause a marked disruption of the neuropil microarchitecture, causing a local loss of SMI-32-positive processes, with a concurrent increase in phosphorylated tau-positive processes (2). Neurites in the vicinity of plaques become dystrophic, with quantitatively altered morphology (3). In our current study, we examined the effect of amyloid-ß deposits on SMI-32 dendrites in transgenic models of amyloid-ß deposition, in which little or no phosphorylated tau occurs in neurites.

We first demonstrate a marked loss of SMI-32-positive dendrites within the vicinity of plaques. Because SMI-32 identifies a population of pyramidal neurons believed to be important for cortical-cortical projections (10), disruption of this population would be expected to reflect functional alterations in neuronal systems that depend upon feedforward and feedback connections among cortical areas. Second, we found that remaining dendrites frequently have an altered morphology. This change in morphology includes an increase in the curvature of the dendrites and an increased length compared to a normal straight

dendrite traversing the same region. This increase in length is graded, and most marked within the boundaries of thioflavine S-positive amyloid-ß deposits. Computer modeling of the functional consequences of these changes suggest marked differences in spike timing in more than a quarter of the remaining dendrites. Thus, there is both a structural loss of dendrites and a predicted functional alteration of remaining dendrites within the vicinity of thioflavine S-positive plaques. In addition, changes in the cytoskeleton in these dystrophic dendrites may have an effect on important cellular functions such as transport of growth factors, protein sorting and targeting, and messenger RNA trafficking. Taken together, these data suggest that the presence of amyloid-ß deposits in the neuropil, especially thioflavine S-positive deposits, might have a direct and profound impact on neural network function.

Several other issues warrant comment. The most substantial alterations in dendrite morphology occur within the confines of thioflavine S-positive amyloid-β plaques, but neurites are not normal for a radius of about 10 to 20 μm surrounding the plaque. We postulate that the cytoskeletal changes that occur to a maximal degree within the amyloid-ß deposit are propagated to some extent proximally and distally. This would tend to worsen the type of functional alterations suggested above, and perhaps provides a framework in which to examine the consequences of amyloid-ß deposits on distal sites.

Finally, comparison of these data with our observations on dendritic geometry associated with senile plaques in human AD reveals many similarities (3). In AD, the greatest changes in dendritic curvature and relative length occur within the confines of amyloid-ß deposits in neurites that contain phosphorylated tau (e.g. curvature = 0.49 μm^{-1}). Neurites that traversed plaques in AD but do not contain Alz-50 immunoreactivity were abnormal (e.g. curvature = 0.30 μm^{-1}), but not as severely changed as the dysmorphic Alz-50 immunoreactive neurites (3). In the APPSw and the PSAPP lines studied here, the extent of alterations is nearly identical to the nonphosphorylated tau containing neurites in AD. Similar observations have been made in PDAPP mice, another line of transgenic mice that overexpress mutant human APP (11). Thus, the current data suggest that transgenic models of amyloid-ß deposition replicate an interesting feature of neuropil disruption due to amyloid deposition also observed in human AD and, in the mouse model, the alteration in dendritic geometry cannot be attributed to the development of phosphorylated tau alterations in the neuronal cell body or cytoskeleton.

Taken together, these results suggest that amyloid-ß deposits are integrally involved in structural and functional alterations in the microarchitecture of the neuropil. Consistent with this idea is the recent observation that somatostatin, substance P, and choline acetyl transferase disappeared in the areas of senile plaque and accumulated in dystrophic neurites around amyloid cores (12). It is not yet known with certainty to what extent amyloid-ß deposits in the neuropil, soluble monomers or oligomers of amyloid-ß, or even overexpression of human amyloid precursor protein itself contributes to behavioral and electrophysiological deficits observed in amyloid precursor protein overexpressing transgenic mice (4, 13, 14). To the extent that our current formulation of direct amyloid-ß induced alterations in the microarchitecture of the neuropil implies distributed neural system dysfunction due to distributed amyloid-ß distribution, therapeutic strategies aimed at preventing or reversing amyloid-ß deposition may have marked positive functional effects (15, 16).

ACKNOWLEDGMENTS

We thank Dr. M. Hasselmo, Boston University, for helpful comments and a critical review of the manuscript. We appreciate the assistance of J. Sanders, E. Kimchi, and S. Sampson.

REFERENCES

1. Hyman BT, Marzloff K, Arriagada PV. The lack of accumulation of senile plaques or amyloid burden in Alzheimer's disease suggests a dynamic balance between amyloid deposition and resolution. J Neuropathol Exp Neurol 1993;52:594–600
2. Knowles RB, Gomez-Isla T, Hyman BT. Abeta associated neuropil changes: Correlation with neuronal loss and dementia. J Neuropathol Exp Neurol 1998;57:1122–30
3. Knowles RB, Wyart C, Buldyrev SV, et al. Plaque-induced neurite abnormalities: Implications for disruption of neural networks in Alzheimer's disease. Proc Natl Acad Sci USA 1999;96:5274–79
4. Hsiao K, Chapman P, Nilsen S, et al. Correlative memory deficits, Aß elevation and amyloid plaques in transgenic mice. Science 1996;274:99–102
5. Duff K, Eckman C, Zehr C, et al. Increased amyloid-beta42(43) in brains of mice expressing mutant presenilin 1. Nature 1996;383: 710–13
6. Irizarry MC, McNamara M, Fedorchak K, Hsiao K, Hyman BT. APPSw transgenic mice develop age-related A beta deposits and neuropil abnormalities, but no neuronal loss in CA1. J Neuropathol Exp Neurol 1997;56:965–73
7. Takeuchi A, Irizarry MC, Duff K, et al. Age-related amyloid beta deposition in transgenic mice overexpressing both Alzheimer mutant presenilin 1 and amyloid beta precursor protein Swedish mutant is not associated with global neuronal loss. Am J Pathol 2000; 157:331–39
8. Bower J, Beeman D. The book of genesis: Exploring realistic neural models with the general neural simulaton system. New York: Springer-Verlag, 1995
9. Yuste R, Tank D. Dendritic integration in mammalian neurons, a century after Cajal. Neuron 1996;16:701–16
10. Campbell MJ, Hof PR, Morrison JH. A subpopulation of primate corticocortical neurons is distinguished by somatodendritic distribution of neurofilament protein. Brain Res 1991;539:133–36
11. Masliah E, Sisk A, Mallory M, Mucke L, Schenk D, Games D. Comparison of neurodegenerative pathology in transgenic mice overexpressing V717F beta-amyloid precursor protein and Alzheimer's disease. J Neurosci 1996;16:5795–811
12. Tomidokoro Y, Harigaya Y, Matsubara E, et al. Impaired neurotransmitter systems by abeta amyloidosis in APPsw transgenic mice overexpressing amyloid beta protein precursor. Neurosci Lett 2000; 292:155–58

13. Hsia AY, Masliah E, McConlogue L, et al. Plaque-independent disruption of neural circuits in Alzheimer's disease mouse models. Proc Natl Acad Sci USA 1999;96:3228–33
14. Larson J, Lynch G, Games D, Seubert P. Alterations in synaptic transmission and long-term potentiation in hippocampal slices from young and aged PDAPP mice. Brain Res 1999;840:23–35
15. Janus C, Pearson J, McLaurin J, et al. A beta peptide immunization reduces behavioural impairment and plaques in a model of Alzheimer's disease. Nature 2000;408:979–82
16. Schenk D, Barbour R, Dunn W, et al. Immunization with amyloid-beta attenuates Alzheimer-disease-like pathology in the PDAPP mouse. Nature 1999;400:173–77

Received February 23, 2001
Revision received April 9, 2001
Accepted April 16, 2001